Cholesterol Sulfate and Ca^{2+} Modulate the Mixing Properties of Lipids in Stratum Corneum Model Mixtures

Marjolaine Arseneault and Michel Lafleur
Department of Chemistry, University of Montreal, Montreal, Quebec H3C 3J7, Canada

ABSTRACT The influence of cholesterol sulfate (CS) and calcium on the phase behavior of lipid mixtures mimicking the stratum corneum (SC) lipids was examined using vibrational spectroscopy. Raman microspectrocopy showed that equimolar mixtures of ceramide, palmitic acid, and cholesterol underwent a phase transition in which, at low temperatures, lipids formed mainly a mosaic of microcrystalline phase-separated domains, and above 45°C, a more fluid and disordered phase in which the three lipid species were more miscible. In the presence of Ca^{2+}, there was the formation of fatty acid-Ca^{2+} complexes that led to domains stable on heating. Consequently, these lipid mixtures remained heterogeneous, and the fatty acid molecules were not extensively involved in the formation of the fluid lipid phase, which included mainly ceramide and cholesterol. However, the presence of CS displaced the association site of Ca^{2+} ions and inhibited the formation of domains formed by the fatty acid molecules complexed with Ca^{2+} ions. This work reveals that CS and Ca^{2+} modulate the lipid mixing properties and the lipid order in SC lipid models. The balance in the equilibria involving Ca^{2+}, CS, and fatty acids is proposed to have an impact on the organization and the function of the epidermis.

INTRODUCTION

The stratum corneum (SC), the top layer of the epidermis, is formed by corneocytes, which are essentially blocks of insoluble keratin resulting from the skin cell migration toward the skin surface. These blocks are held together by lipid layers. To provide a tight skin barrier, the lipid structure joining the corneocytes must be highly cohesive. However, the skin is continuously renewed, and at the surface, there is the loss of cohesion and shedding of individual corneocytes (1,2), a phenomenon called desquamation. Because the lipid phase is believed to ensure cell cohesion, desquamation is likely related to some changes in the structural properties of these lipids (3–5). Chemical changes occur during the skin migration toward the surface. For example, cholesterol sulfate (CS) present in the epidermis is enzymatically degraded in cholesterol by steroid sulfatase before its arrival at the SC level (3,6,7). Similarly a Ca^{2+} gradient exists through the epidermis, and it has been associated with cellular terminal differentiation, barrier function, and desquamation (8–12).

In the work presented here, the impact of CS and Ca^{2+} on the behavior of model lipid mixtures mimicking the SC lipids was examined using vibrational spectroscopy. Equimolar mixtures of ceramide, cholesterol, and fatty acid have been widely used as SC model mixtures because these three lipids are the main lipidic species found in the SC(6,13,14). Nonhydroxylated ceramides are the most abundant class of ceramides found in SC (14) and, consequently, are often used in these model mixtures. Ceramide III (CerIII), enzymatically prepared from sphingomyelin extracted from bovine brain, is equivalent to skin nonhydroxylated ceramide, even though the chain composition may be slightly different (15). Fatty acids in the SC are typically saturated and bear long chains, between C_{16}, and C_{28}, with C_{22} and C_{24} being the most abundant (13,16–18). Palmitic acid (PA) has often been selected as a generic fatty acid and was used in the study presented here because the phase behavior of SC lipid model mixtures containing PA is, at this point, best characterized by several techniques. Moreover, the use of palmitic acid with a perdeuterated acyl chain (PA-d_{31}) makes it possible to distinguish spectroscopically the behavior of the fatty acid acyl chain from that of CerIII. Model mixtures based on mixtures of CerIII, PA-d_{31}, and cholesterol were selected in this study. These mixtures showed a dominant lamellar periodicity of 5.38 nm at room temperature (19). Typically x-ray diffraction on SC has shown the existence of two lamellar spacings at ~6 and ~13 nm (20–22). The lack of the long-periodicity phase in the model mixtures used in this study is probably associated with the use of a single ceramide. It has been shown recently that more complex mixtures that include at least three ceramide types could reproduce both lamellar spacings (23–25). Despite this difference, the simple model mixtures have been shown to reproduce several features of the SC lipids. At low temperature, they exhibit a high proportion of crystalline lipids and an orthorhombic chain packing analogous to those observed in SC lipids (22,26–28). On heating, the acyl chains of CerIII and PA undergo transitions toward disordered phases between 45 and 65°C (27–29), a feature also consistent with the DSC thermograms of the SC lipids (30–32).

The behaviors of CerIII/PA-d_{31}/cholesterol and CerIII/PA-d_{31}/CS mixtures were compared in the presence and the

Submitted May 29, 2006, and accepted for publication September 8, 2006.

Address reprint requests to Michel Lafleur, Dept. of Chemistry, University of Montreal, CP 6128, Succ. Centre Ville, Montreal, Quebec H3C 3J7, Canada. Tel.: 514-343-5936; Fax: 514-343-7586; E-mail: michel.lafleur@umontreal.ca.

0006-3495/07/01/99/16 $2.00

doi: 10.1529/biophysj.106.090167

absence of Ca^{2+} to highlight the impact of electrostatic modification on the phase behavior of these systems. CS is a minor component of the SC. It represents ~2% (w/w) of the SC lipids, and the CS/free sterol ratio is ~0.14 (3,5,18). Despite its low concentration, CS was proposed to play essential functions in several skin processes including differentiation, cholesterol metabolism, and desquamation (5,7,33,34). More specifically, it has been proposed that CS plays a critical role in desquamation on the basis of the perturbation in the SC lipid composition of people suffering with the X-linked recessive ichthyosis (7,35,36). The desquamation process of these people is severely inhibited, and large scales, formed by the accumulation of SC, are present on their body. The genetic defect associated with the disease leads to a deficit in steroid sulfatase, which, as mentioned above, is responsible for the transformation of CS in cholesterol. Consequently, this ichthyosis is accompanied by the accumulation of CS in the SC and a decrease of the cholesterol content. CS, in the case, constitutes ~12% (w/w) of the SC lipids, and the CS/free sterol ratio increases by a factor 10, reaching ~1 (7). These observations suggest that the presence of CS in the SC, or a high CS/cholesterol ratio, may drastically inhibit the desquamation by stabilizing the lamellar phases in the deep layers of the SC. The comparison between the behavior of CerIII/PA-d_{31}/chol and CerIII/PA-d_{31}/CS mixtures should lead to insights into the impact of this molecular sterol modification in the SC lipid structural properties.

The behavior of CerIII/sterol/PA mixtures was investigated in the presence of Ca^{2+} because of the key role of this cation in modulating the SC structure. The presence of Ca^{2+} was found to be essential for the skin barrier and differentiation (9,11,37–39). The concentration of Ca^{2+} displays a gradient with a complex shape across the epidermis, increasing from the basal layer to reach a maximum at the stratum granulosum layer and decreasing abruptly in the SC (8–11). It has been proposed that Ca^{2+} plays a fundamental role in the stability of SC lipids. For example, Ca^{2+} could bridge adjacent lipid layers via its interaction with the negatively charged sulfate group of CS (40), a proposed contribution to the enhanced cohesion of SC lipids in the case of the X-linked recessive ichthyosis. The characterization of the impact of Ca^{2+} on skin lipid structure is limited. Up to now, it has been suggested, on the basis of small-angle x-ray diffraction, that Ca^{2+} counterbalances the ability of CS to solubilize cholesterol in the SC lipid matrix (34).

Infrared (IR) and Raman spectroscopies have been used to characterize the behavior of the mixtures. IR spectroscopy is a well-established technique providing information relative to the acyl chains as well as the polar head group (27,28,41–44). Complementary information has been obtained from Raman spectroscopy. It has been shown that Raman microspectroscopy was particularly useful for the study of the SC model mixtures as crystalline domains in the order of tens of micrometers were observed, and chemical imaging revealed the heterogeneous distribution of the lipids on the microscopic scale (45).

MATERIALS AND METHODS

CerIII (99%), cholesterol (99%), CS, 2-[*N*-morpholino]ethanesulfonic acid (MES), and D_2O (99%) were purchased from Sigma Chemical (St. Louis, MO). PA-d_{31} was obtained from CDN Isotopes (Pointe-Claire, Quebec, Canada). NaCl was provided by Anachemia (Montreal, Quebec, Canada).

To produce homogeneous mixtures, the lipids were individually solubilized in a benzene/MeOH solution (95:5, v/v) except for CS, which was solubilized in a 25:75 mixture. Appropriate amounts of the lipid solutions were mixed to obtain the desired molar ratio. The lipid organic solutions were then freeze-dried for at least 16 h. The resulting lipid powder was hydrated with a MES buffer (100 mM MES, 100 mM NaCl), pD 5.2, a value representative of the SC pH (46,47). The buffer was prepared in D_2O, to avoid water contribution in the amide I' region. For the Ca^{2+}-free samples, 5 mM EDTA was present in the buffer. For the Ca^{2+}-containing sample, $CaCl_2$ (100 mM) was present in the buffer. For the mixtures including cholesterol, the buffer was added in large excess (a lipid/buffer ratio of 1% (w/v)) to provide an easy control of the pH. These mixtures led to waxy particles with no detectable lipids in the supernatant. For the mixtures including CS, the final lipid concentration in the buffer was 20% (w/v), as these mixtures led to homogeneous suspensions. Three freeze-and-thaw cycles, from liquid nitrogen to 80°C, were imposed on the samples. Subsequently, the samples were centrifuged 30 min at 3500 × *g*. Annealing periods between 2 and 4 h, at 30°C, were performed on all samples to favor the thermodynamically stable phase. It was shown that the behavior of ceramide-containing samples is sensitive to their thermal history (27,48,49). Because these systems can form solid phases at low temperature, it is necessary to provide the appropriate conditions leading to the solidification of the lipids to obtain reproducible results.

IR spectra were obtained according to an established procedure (27,41). Briefly, the spectra were obtained by transmission, from an aliquot put in a cell with CaF_2 windows, a path length of 5 μm, and whose temperature was controlled with Peltier elements. They were recorded on an FTS-25 BioRad spectrometer equipped with a water-cooled globar source, a KBr beam splitter, and a mercury-cadmium-telluride detector. Each spectrum was the result of 100 scans, with a nominal resolution of 2 cm^{-1}, Fourier-transformed with a triangular apodization. The spectra were recorded as a function of increasing temperature. To determine the position of the bands associated with the symmetric stretching of the methylene groups, the spectral contribution of D_2O was first eliminated from the C-H stretching modes and the C-D stretching modes by simulating the edge of the O-D stretching band with a polynomial of order 3, independently for these two regions. The reported positions correspond to the gravity centers of the top 5% of the bands.

The Raman spectra were acquired on a Renishaw Raman Imaging Wire 3000 system (Gloucestershire, UK), equipped with a Leica LM microscopy (Deerfield, IL), a long focal distance ×50 lens, and a charge-coupled device camera (600 × 400). Only four pixel rows (600 × 4) were used for recording the spectra; this approach provided a virtual pinhole and allowed us to work in confocal conditions, leading to a spatial resolution of ~5 μm along the *z*-axis (perpendicular to the platform). The Ar^+ laser, with 15 mW at the sample, had a beam diameter of ~2 μm, as estimated from its reflection on a silicon surface. A computer-controlled platform (ProScan, Prior Scientific Instruments, Fulbourn, UK) was used for the chemical mapping. An aliquot of the lipid mixture was deposited on a quartz window that served as the top cover of the sample holder. The cell was filled with water to maintain full hydration, then sealed. The temperature control was ensured by heating elements inserted in the aluminum base of the cell. Typically a 40 × 40 μm^2 surface was swept, with 3-μm steps, recording Raman spectra between 1900 and 3200 cm^{-1}. These conditions led to 14 × 14 or 196 spectra per map. The total time for recording a map was ~3 h. The same region was scanned as a

function of increasing temperature, from 25 to 75°C. An equilibration delay of 10 min was used between successive temperatures.

The maps were generated using GRAMS/32 (Galactic Industries Corporation, Salem, NH), and WIRE (Renishaw, Gloucestershire, UK) software. The intensities were measured from the baseline to the Raman scattering intensity at the given wave number. The width at half-height of the C-D symmetric stretching band ($\Delta\nu_{CD}$) was measured on the fitted band at ~2100 cm^{-1} resulting from a band fitting of the region between 2070 and 2160 cm^{-1}, using three components.

RESULTS

Fig. 1 shows the thermotropism of the SC model mixtures as probed by the C-H symmetric stretching mode of the methylene (ν_{CH}) and the C-D symmetric stretching mode of the CD_2 groups (ν_{CD}) from the IR spectra. The position of these bands is known to be sensitive to the conformation order of the acyl chains (27,28,50,51). The ν_{CH} position was used to report the chain order of CerIII, as the contribution of cholesterol in this region does not significantly affect the band position and, in addition, remains practically constant during the temperature variation (27,52). The ν_{CD} position describes the chain order of PA-d_{31}. The thermotropism of the CerIII/PA-d_{31}/chol mixture, obtained from these two spectral parameters, is well established (27,28) and was reproduced in this study for the sake of comparison. At low temperature, the positions of ν_{CH}, and ν_{CD} were 2848, and 2089 cm^{-1}, respectively, and these values are typical of highly ordered chains (27,28,44). On heating, both bands experienced a shift toward high frequency between 40 and 65°C. This shift indicated a disordering of the acyl chains of both CerIII and PA-d_{31}. A point of inflection was observed on both curves at ~50°C. At this point, the ν_{CH}, and the ν_{CD} positions were 2851, and 2092 cm^{-1}, respectively, in agreement with previous results (27). These values are typical of those obtained for a liquid ordered phase (27,53,54). The thermal behavior of this system has been associated with a transition from a solid to a liquid ordered phase followed by the formation of a disordered and isotropic phase on further heating (27–29,41,49,55). The thermotropism of this mixture was drastically modified by the presence of Ca^{2+} (Fig. 1 *B*). Below 40°C, the positions of ν_{CH}, and ν_{CD} bands were 2849 and 2090 cm^{-1}, typical of highly ordered chains. On heating, the ν_{CH} band was shifted between 40 and 50°C to ~2851 cm^{-1}. This value suggested that some acyl chain conformational disorder has been thermally induced, but the chains remained, on average, more ordered than a typical fluid disordered phase, for which the ν_{CH} band is around 2854 cm^{-1} (27,28,50). At 60°C, the band was shifted again to reach ~2853 cm^{-1} at 75°C. The shift did not level off suggesting that the transition would be completed at a temperature higher than that accessible with our experimental setup. In contrast, the ν_{CD} position was practically constant over the whole temperature variation, indicating that the PA-d_{31} acyl chain remained highly ordered in the presence of Ca^{2+} despite heating up to 75°C.

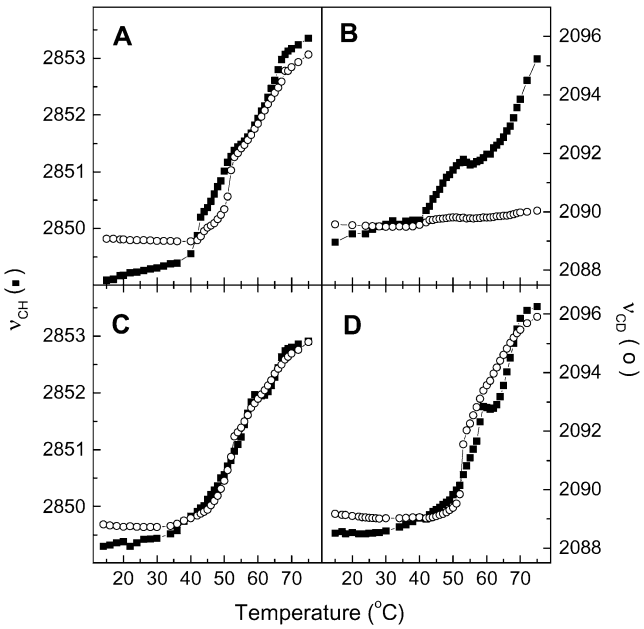

FIGURE 1 Thermotropism of CerIII/PA-d_{31}/sterol (1:1:1) mixtures, as probed by the methylene stretching mode by IR spectroscopy. (*A*) CerIII/PA-d_{31}/chol (1:1:1) mixtures free of Ca^{2+}. (*B*) CerIII/PA-d_{31}/chol (1:1:1) mixtures with 100 mM Ca^{2+}. (*C*) CerIII/PA-d_{31}/CS (1:1:1) mixtures free of Ca^{2+}. (*D*) CerIII/PA-d_{31}/CS (1:1:1) mixtures with 100 mM Ca^{2+}. The two *y*-scales were adjusted such that a gel-to-liquid crystalline phase transition of phospholipid bilayers is represented by a variation with the same amplitude for the two parameters. (■) ν_{CH} and (○) ν_{CD}.

The thermotropism of the CerIII/PA-d_{31}/CS mixture is also displayed in Fig. 1. Overall, the behavior of this mixture, in the presence and the absence of Ca^{2+}, was reminiscent of that of the CerIII/PA-d_{31}/chol mixture free of Ca^{2+}. Below 40°C, the position of ν_{CH} and ν_{CD} bands were typical of solid phases (2849 and 2089 cm^{-1}, respectively). Between 40 and 65°C, the bands experienced a shift toward 2853 and 2096 cm^{-1}, respectively. Therefore, it is concluded that the acyl chains of both CerIII and PA-d_{31} underwent a transition from a solid to a fluid disordered phase, irrespective of the presence of Ca^{2+}. These band shifts were not monotonous, and the details appeared to be slightly different with and without Ca^{2+}. For example, the order-disorder transition appeared more abrupt and at a slightly higher temperature in the presence of CS than in the mixtures with cholesterol.

The description of the interfacial groups by IR spectroscopy revealed a key change in the association of Ca^{2+} with the SC model mixtures (Fig. 2). The C=O stretching of the carboxylic group (ν_{COOH}) was located between 1670 and 1700 cm^{-1}, whereas the C–O symmetric stretching of the carboxylate ($\nu_{COO}-$) bands appeared between 1500 and 1580 cm^{-1}. In the case of the CerIII/PA-d_{31}/chol mixture free of Ca^{2+}, only the ν_{COOH} bands were observed indicating that, in these conditions, the fatty acid was completely protonated. This finding is in agreement with the previous determination of the pK_a of fatty acids reconstituted in lipid matrices, estimated

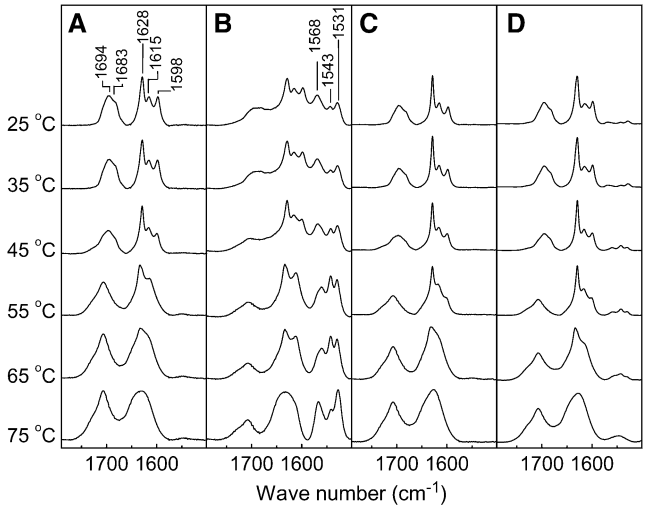

FIGURE 2 Thermal evolution of the amide I', ν_{COOH}, and ν_{COO}- bands for SC model mixtures. (*A*) CerIII/PA-d_{31}/chol (1:1:1) mixtures free of Ca^{2+}. (*B*) CerIII/PA-d_{31}/chol (1:1:1) mixtures with 100 mM Ca^{2+}. (*C*) CerIII/PA-d_{31}/CS (1:1:1) mixtures free of Ca^{2+}. (*D*) CerIII/PA-d_{31}/CS (1:1:1) mixtures with 100 mM Ca^{2+}. Temperatures are indicated on the left.

to be between 6.3 and 8.7 (56–58). The shape of the ν_{COOH} bands and their thermal evolution reproduced previous results (27). At low temperature, the band included a main component at 1694 cm^{-1} with a shoulder at 1683 cm^{-1}. The band shape and position were analogous to those obtained from solid fatty acids and even more similar to fatty acid/cholesterol mixtures forming phase-separated crystalline domains (59). On heating, the ν_{COOH} band was shifted toward higher frequency and lost its shoulder at 1683 cm^{-1}. These changes are indicative of the melting of solid PA-d_{31} (27,41,59). The amide I' band showed three components at 1628, 1615, and 1598 cm^{-1}, and these were associated with different H bond patterns at the interface (27,41). The 1598 cm^{-1} component disappeared between 45 and 55°C, and the two other components, at 1628 and 1615 cm^{-1}, merged, leading to a broad band between 60 and 70°C. These variations correlated well with those observed in the ν_{CH} region. They were associated with the solid-liquid ordered phase transition and the subsequent liquid ordered-disordered phase transition, as discussed in detail previously (27,29,41,49,55). In the presence of Ca^{2+}, the most striking features are the three additional components, at 1568, 1543, and 1531 cm^{-1}, observed in the ν_{COO}- region of the IR spectra. This profile was more complex than that obtained for unprotonated PA in phospholipid matrices (57,60) and in PA/chol bilayers (61). Two of the three components, those at 1568 and 1531 cm^{-1}, have been observed for calcium stearate and were assigned to the carboxylate asymmetric stretch of carboxylate groups coordinated with Ca^{2+} in different modes (62–65). A contribution of the ν_{COOH} band, at 1685 cm^{-1} was also observed, indicating the coexistence of the protonated PA and the PA-Ca^{2+} complex, in these conditions. The ratio of the ν_{COO}- band area over the sum of those of the ν_{COO}- and ν_{COOH} bands was ~0.6. The variations of the amide I' and ν_{COOH} band shape as a function of heating were similar to that observed for the mixture in the absence of Ca^{2+}. The ν_{COO}- bands remained a main component of this region over the whole temperature range, with small changes in the position and relative intensity of its components.

The region of the IR spectra associated with the interfacial groups for the CerIII/PA-d_{31}/SC mixture is also displayed in Fig. 2, *C* and *D*. For the CS-containing mixtures with and without Ca^{2+}, the thermal evolution behavior of these bands was found to be analogous to that of the CerIII/PA-d_{31}/chol mixture in the absence of Ca^{2+}, the main differences being the changes occurring at slightly different temperatures.

These mixtures were characterized by Raman microspectroscopy because this technique allowed us to get information relative to the spatial lipid distribution, with a resolution sufficient to observe phase-separated domains in the SC mixtures (45). The main investigated regions were the C-H stretching (2800–3000 cm^{-1}) and the C-D stretching (1900–2250 cm^{-1}) regions (Fig. 3). As described below, their relative intensities are representative of the lipid composition of the mixture in the sampled volume. In addition, these regions, similarly to those recorded in IR spectroscopy, carry some information about the conformation chain order (66–68). In the C-D stretching region, the main band located at ~2100 cm^{-1} is assigned to the C-D symmetric stretching of the PA-d_{31} acyl chain. Its width is associated with the conformational order of the acyl chain. It was observed that

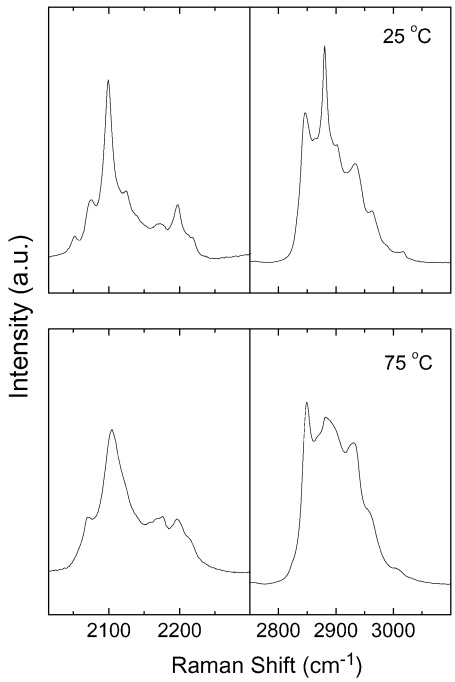

FIGURE 3 Raman spectra of CerIII/PA-d_{31}/chol (1:1:1) mixtures free of Ca^{2+}, at 25 and 75°C.

the heating of the CerIII/PA-d_{31}/chol mixture led to a significant broadening of this band for which the width at half-height ($\Delta\nu_{CD}$) increased from 14 to 30 cm^{-1} between 25 and 75°C (Figs. 3 and 4). Similarly, the C-H stretching region of the Raman spectra underwent characteristic changes during the disordering of the hydrogenated acyl chains. The bands at 2850 and 2880 cm^{-1} were assigned, respectively, to the symmetric and antisymmetric C-H stretching of methylene groups. It has been shown that their intensity ratio (I_{2880}/I_{2850}) is mainly sensitive to vibrational coupling between ordered hydrogenated acyl chains and therefore constitutes a probe of the conformational order of the acyl chains (66,67,69). As seen in Fig. 3, the I_{2880}/I_{2850} of CerIII/PA-d_{31}/chol mixtures decreased drastically when the temperature increased from 25 to 75°C. It should be noted that cholesterol contributed in the region. Its most intense contribution was at 2935 cm^{-1}: this feature could be observed in the spectra of CerIII/PA-d_{31}/chol mixtures. As discussed below, the contribution of cholesterol appeared to be rather independent of the temperature.

The overall behavior of the SC mixtures was characterized by the mean Raman spectra obtained from the addition of the 196 spectra associated to a map, recorded at a given temperature, over an area of $40 \times 40\ \mu m^2$ of the sample. The reproducibility of these average spectra for different maps confirmed that the sampled areas were sufficiently large to be representative of the samples. The evolution of the chain order, as described by the I_{2880}/I_{2850} ratio for CerIII and the $\Delta\nu_{CD}$ for PA-d_{31} (Fig. 4), was consistent with the results obtained from IR spectroscopy. The I_{2880}/I_{2850} ratios measured for the CerIII/PA-d_{31}/chol mixture free of Ca^{2+} decreased on heating from 1.5 at 25°C, to 0.9 at 75°C. When these values were corrected for the contribution of cholesterol, using its contribution at 2935 cm^{-1} to estimate the subtraction factors, the value at 25°C became 1.4, whereas the value at 75°C remained at 0.9. The low-temperature values were typical of highly ordered chain, whereas the high-temperature values were typical of disordered chains (67,70). The $\Delta\nu_{CD}$ values increased on heating from 13 to 30 cm^{-1}, a change representative of a transition from highly ordered to disordered alkyl chains (68,71). The variations were observed between 40 and 65°C for both parameters and consequently indicated that both CerIII and PA-d_{31} acyl chains disordered in a concomitant manner on heating. The presence of Ca^{2+} modified the behavior of the CerIII/PA-d_{31}/chol mixtures, in agreement with the IR results. The progression of the I_{2880}/I_{2850} ratios was not considerably affected by Ca^{2+}, but the presence of the cation led to a much more limited variation of the $\Delta\nu_{CD}$ values ($\sim$5 cm^{-1}). These results confirm that PA-d_{31} remained mostly ordered up to 75°C when Ca^{2+} was present, whereas CerIII underwent melting. The thermotropism of the CerIII/PA-d_{31}/CS mixture with and without Ca^{2+}, as reported from the I_{2880}/I_{2850} ratios and $\Delta\nu_{CD}$, was similar to that obtained for the CerIII/PA-d_{31}/chol mixture in the absence of Ca^{2+}. Both parameters reflected a disordering of the alkyl chains of CerIII and PA-d_{31} on heating from 35 to 65°C.

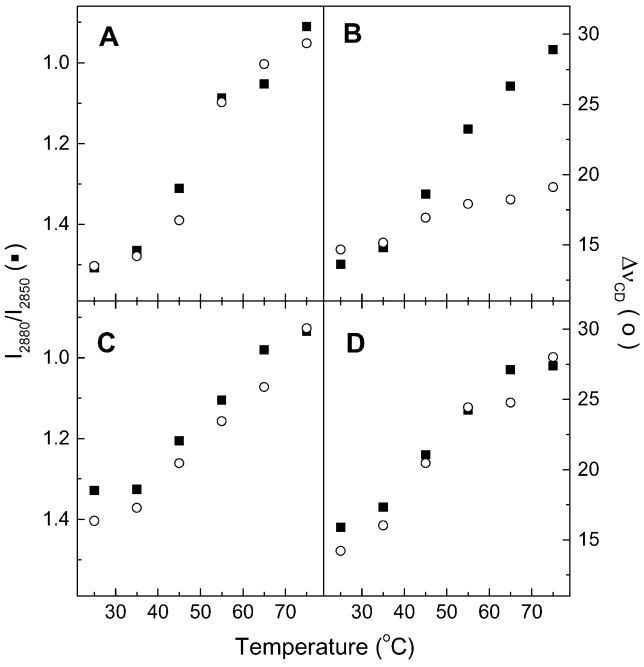

FIGURE 4 Thermotropism of CerIII/PA-d_{31}/sterol (1:1:1) mixtures, as probed by the I_{2880}/I_{2850} intensity ratios (■) and the $\Delta\nu_{CD}$ (○) obtained from Raman spectroscopy. (*A*) CerIII/PA-d_{31}/chol (1:1:1) mixtures free of Ca^{2+}. (*B*) CerIII/PA-d_{31}/chol (1:1:1) mixtures with 100 mM Ca^{2+}. (*C*) CerIII/PA-d_{31}/CS (1:1:1) mixtures free of Ca^{2+}. (*D*) CerIII/PA-d_{31}/CS (1:1:1) mixtures with 100 mM Ca^{2+}. The two *y*-scales were adjusted such that a gel-to-liquid crystalline phase transition of phospholipid bilayers is represented by a variation with the same amplitude for the two parameters. Note that the I_{2880}/I_{2850} scale is upside down to allow the direct comparison with the $\Delta\nu_{CD}$ variations.

The Raman chemical mapping provided the spatial distribution of the different lipid species in the sample. The ratio of the area of the C-D stretching region ($A_{\nu CD}$) over the sum of ($A_{\nu CD} + A_{\nu CH}$), where $A_{\nu CH}$ is the area of the C-H stretching region, was used to describe the proportion of PA-d_{31} relative to the three lipid components in the sampling elements (Figs. 5–8). The integrating limits were from 2015 to 2250 cm^{-1} and from 2780 to 3100 cm^{-1} for the $A_{\nu CD}$ and $A_{\nu CH}$, respectively. The band at 2935 cm^{-1} is a main feature in the spectra of cholesterol, whereas the band at 2850 cm^{-1} in the Raman spectra of pure CerIII showed very limited changes on heating. Therefore, the intensity ratio of these features ($I_{2850}/(I_{2850} + I_{2935})$) was used to represent the proportion of CerIII relative to CerIII and cholesterol or, in other words, to describe the lipid composition excluding PA-d_{31}. This ratio, derived from the spectra at 25°C, was found to be 0.67 and 0.46 for pure CerIII and pure cholesterol, respectively. The ratio varied from 0.67 to 0.61 when pure CerIII was heated from 25 to 75°C. Consequently, the variations of this ratio mainly (but not exclusively) reported changes in the relative CerIII and cholesterol proportions.

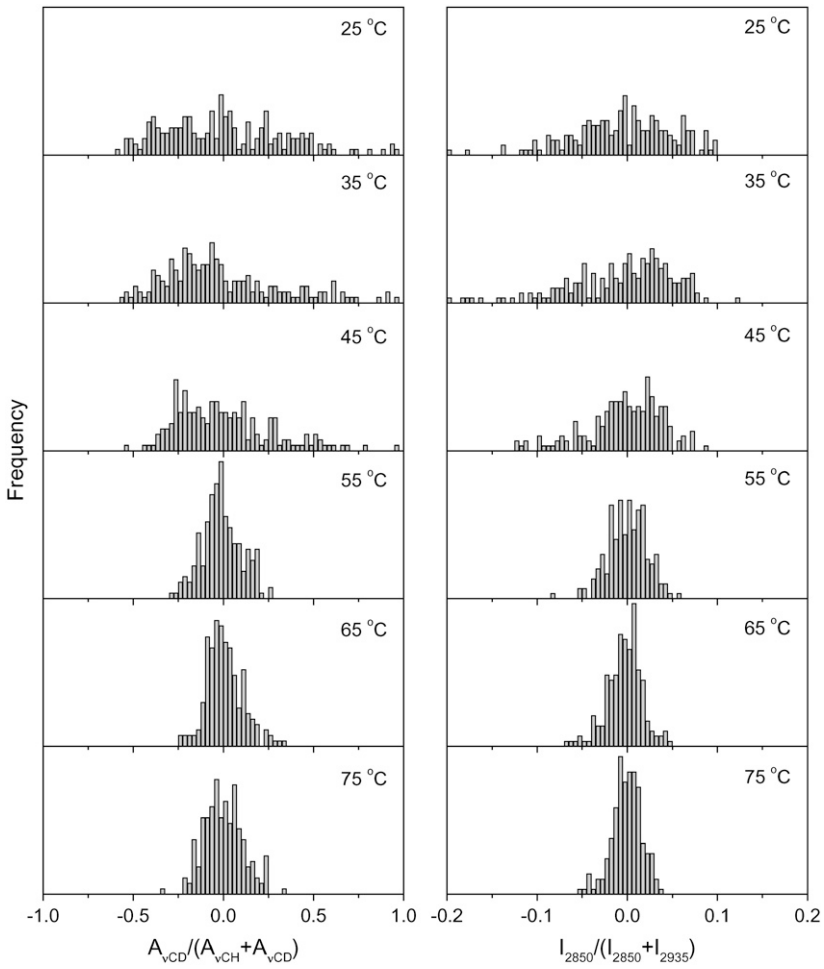

FIGURE 5 Normalized lipid spatial distributions in the CerIII/PA-d_{31}/chol (1:1:1) mixtures free of Ca^{2+}. (*Left*) $A_{\nu CD}/(A_{\nu CD} + A_{\nu CH})$ representing the distribution of PA-d_{31} relative to (CerIII/PA-d_{31}/chol). (*Right*) $I_{2850}/(I_{2850} + I_{2935})$ representing the distribution of CerIII relative to (CerIII/chol). The *y*-scale was kept the same for the parameter distributions at different temperatures.

The absolute values of I_{2850}, I_{2935}, $A_{\nu CD}$, and $A_{\nu CH}$ and, as a consequence, the absolute values of the derived parameters described above were dependent on the temperature mainly because of its influence on the lipid structure. This dependence was nonlinear. Because the samples were heterogeneous from a composition and chain order point of view, it was not possible to simulate all the spectra from those obtained with the pure lipid species, preventing a detailed quantitative analysis. Therefore, the spectral ratios defined above were normalized relative to the value that was measured on the mean spectra, averaged over the whole map, $((x_i - x_{mean})/x_{mean})$. Consequently, values above 0 represent sampling elements enriched in a species, whereas negative values are representative of depleted sampling elements, relative to the average proportion. This approach provides a straightforward illustration of the evolution of the heterogeneity in the samples as a function of temperature. Fig. 5 displays the evolution of the spatial composition distribution of the CerIII/PA-d_{31}/chol mixture as a function of temperature. At 25°C, the PA-d_{31} proportion, as described by $A_{\nu CD}/(A_{\nu CD} + A_{\nu CH})$, showed a broad distribution, with some sampling elements significantly enriched or depleted compared to the average value. Similarly, the CerIII proportions, described by $I_{2850}/(I_{2850} + I_{2935})$ were also found to be broadly distributed. These results are fully consistent with those previously reported by vibrationnal spectroscopy (42,45). At 25°C, the Raman spectra were essentially composed of those of the three pure compounds in the solid form. Therefore, a more quantitative analysis of the composition could be performed, according to a method previously published (45). That analysis led to the molar fractions of each species in the mixtures, and, in agreement with the previous study (45), the molar fractions of CerIII, PA-d_{31}, and cholesterol varied between 0.1 and 0.6, the average fraction being 0.33 for these components. The distributions of the two spectral parameters were similar at 35°C. When the samples were heated at 45°C and above, the width of the composition distribution of both species was considerably reduced, the most pronounced variation being observed between 45 and 55°C, corresponding to the first part of the transition probed by IR spectroscopy (Fig. 1). The homogenization of the mixture revealed by these results is therefore concomitant with the chain disordering previously inferred from the IR and Raman spectroscopy results. At 75°C, the distribution

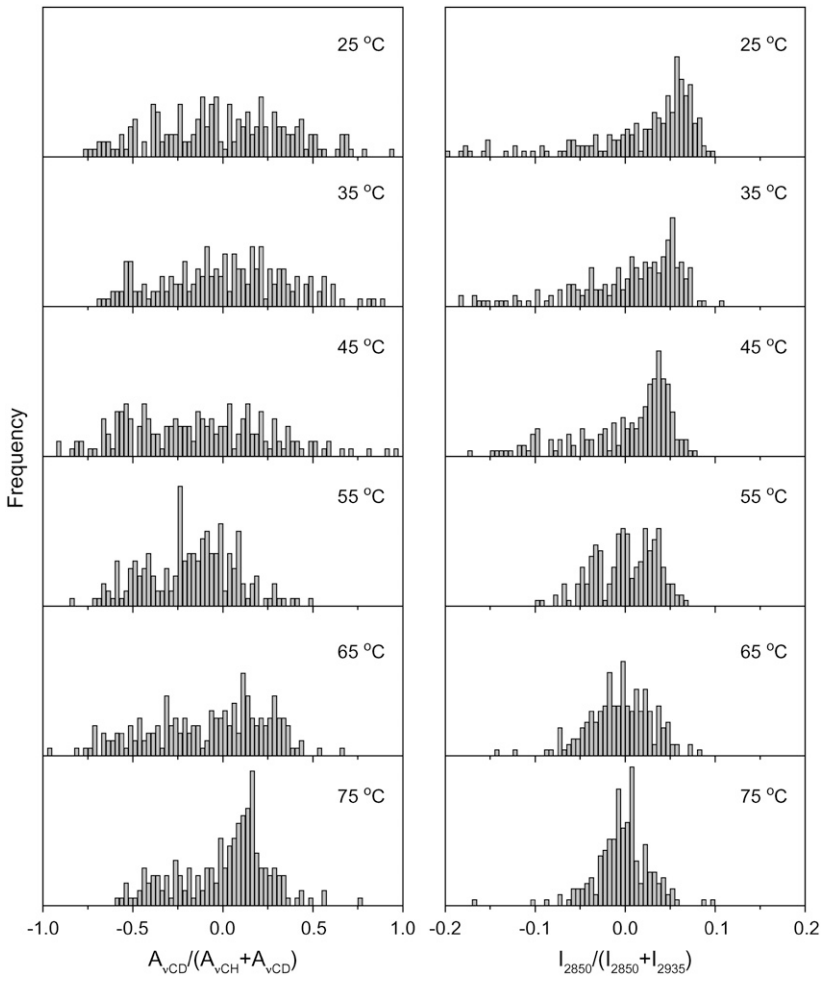

FIGURE 6 Normalized lipid spatial distributions in the CerIII/PA-d_{31}/chol (1:1:1) mixtures with 100 mM Ca^{2+}. (*Left*) $A_{\nu CD}/(A_{\nu CD} + A_{\nu CH})$ representing the distribution of PA-d_{31} relative to (CerIII/PA-d_{31}/chol). (*Right*) $I_{2850}/(I_{2850} + I_{2935})$ representing the distribution of CerIII relative to (CerIII/chol). The *y*-scale was kept the same for the parameter distributions at different temperatures.

widths of both parameters were relatively narrow but still significantly broader (by a factor of ~2) than those obtained for freeze-dried CerIII/PA-d_{31}/chol mixtures, which should correspond to a completely homogeneous mixture.

The spatial composition distribution of the CerIII/PA-d_{31}/chol mixture in the presence of Ca^{2+} is presented in Fig. 6. Between 25 and 45°C, the composition distributions of both PA-d_{31} and CerIII were found to be broad and representative of heterogeneous samples. On further heating, the distribution of PA-d_{31} in the mixture remained broad, whereas that of CerIII became progressively narrower. Therefore, it is concluded that the distribution of PA-d_{31} remained inhomogeneous over the whole investigated temperature range. At temperatures lower than 45°C, the distributions of CerIII and cholesterol were also heterogeneous but became more homogeneous on heating (Fig. 6, *right column*). This homogenization corresponded to the CerIII acyl chain disordering observed by IR (Fig. 1) and Raman (Fig. 4) spectroscopy.

The composition distributions of CerIII and PA-d_{31} for the CerIII/PA-d_{31}/CS mixture in the absence and the presence of Ca^{2+} are presented in Figs. 7 and 8, respectively. These distributions were analogous to those obtained for CerIII/PA-d_{31}/chol mixtures in the absence of Ca^{2+}. At low temperature, the spatial distributions of PA-d_{31} and CerIII were broad, illustrating phase-separated samples. They became considerably narrower on heating, indicating a more uniform spatial lipid distribution. This homogenization was, as mentioned for the other mixtures, concomitant with the disordering of the lipid acyl chains.

The spatial distributions of PA-d_{31} and CerIII in the CerIII/PA-d_{31}/sterol mixtures, in the presence of 100 mM Ca^{2+}, are represented on the chemical maps in Fig. 9. In the top panels (Fig. 9 *A*), the distribution of PA-d_{31} is represented by the normalized values of $A_{\nu CD}/(A_{\nu CD} + A_{\nu CH})$: bright red pixels represent elements enriched in PA-d_{31}, whereas bright blue ones indicate elements enriched in CerIII and/or sterol. At low temperature, the pixels with bright colors were indicative of the formation of domains with specific lipid composition. The size of these domains was on the order of micrometers, in agreement with previous results obtained on these mixtures in the absence of Ca^{2+} (42,45). The domains showed, however, a wide range of size and undefined shapes. Similarly, the maps obtained from $I_{2850}/(I_{2850} + I_{2935})$ also indicated the presence of sampling

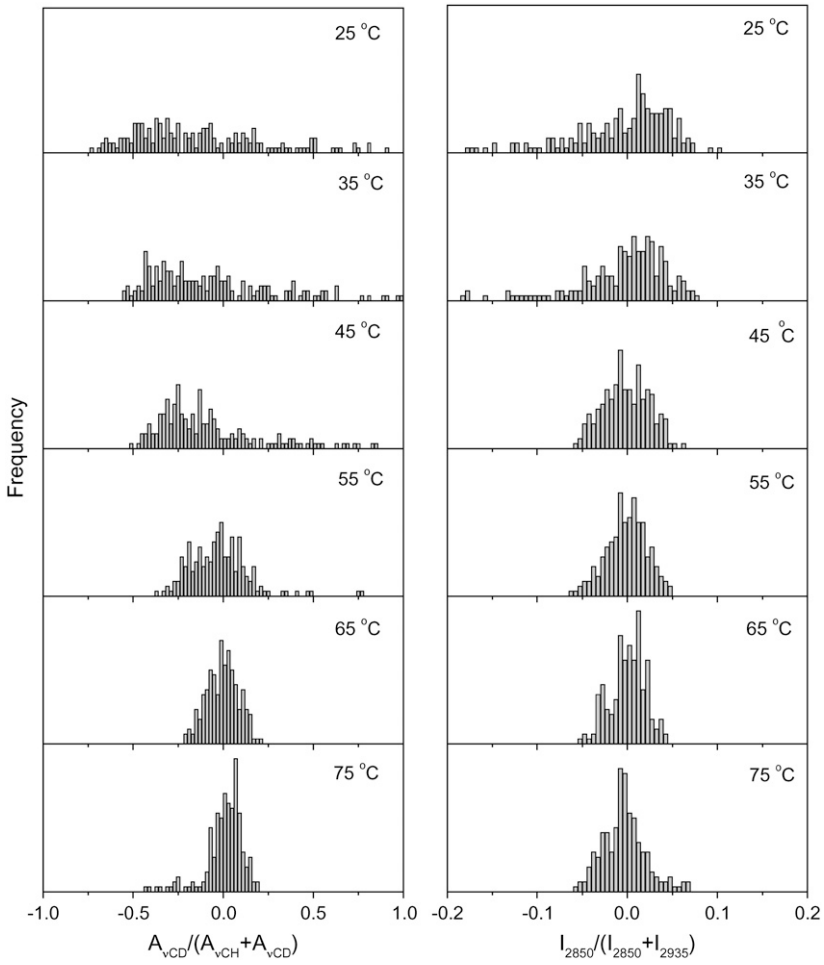

FIGURE 7 Normalized lipid spatial distribution in the CerIII/PA-d_{31}/CS (1:1:1) mixtures free of Ca^{2+}. (*Left*) $A_{\nu CD}/(A_{\nu CD} + A_{\nu CH})$ representing the distribution of PA-d_{31} relative to (CerIII/PA-d_{31}/CS). (*Right*) $I_{2850}/(I_{2850} + I_{2935})$ representing the distribution of CerIII relative to (CerIII/CS). The *y*-scale was kept the same for the parameter distributions at different temperatures.

elements enriched in CerIII relative to cholesterol (*bright green pixels*) as well as elements enriched in cholesterol relative to CerIII (*bright white pixels*). These results indicate that the samples were, at low temperatures, formed by a mosaic of domains mainly enriched in one component. The homogenization of the spatial distribution of CerIII observed on heating the CerIII/PA-d_{31}/chol mixtures in the presence of Ca^{2+} is clearly observed on the chemical maps (Fig. 9 *A*); most of the pixels became gray or light green, indicative of values close to the mean values. On the other hand, the distribution of PA-d_{31} remained fairly heterogeneous. In the presented maps, even at high temperatures, some sampling elements were considerably enriched compared to the average value (*bright red pixels*), but a considerable number of pixels showed depletion in fatty acid (*bright blue pixels*). Some of the later elements, for example, formed a domain observable in the bottom left corner. This domain was present during the whole temperature variation.

For comparison, the chemical maps obtained from CerIII/PA-d_{31}/CS mixture in the presence of Ca^{2+} are also presented (Fig. 9 *B*). At low temperature, bright pixels could be observed on the maps derived from the $A_{\nu CD}/(A_{\nu CD} + A_{\nu CH})$ and $I_{2850}/(I_{2850} + I_{2935})$, indicating the presence of microdomains. On heating, the pixels became duller, illustrating the disappearance of lipid domains that happened in parallel to the chain melting. The chemical maps, obtained between 25 and 75°C, for CerIII/PA-d_{31}/chol, and CerIII/PA-d_{31}/CS mixtures in the absence of Ca^{2+} (data not shown) were similar to those presented for CerIII/PA-d_{31}/CS mixtures with Ca^{2+}.

The lipid chain order could also be spatially described using the I_{2880}/I_{2850} and $\Delta\nu_{CD}$ values as discussed above. Their distributions are presented in Fig. 10. At 25°C, the I_{2880}/I_{2850} and the $\Delta\nu$CD values obtained for the CerIII/PA-d_{31}/chol mixture in the presence of 100 mM Ca^{2+} showed quasi normal distributions centered around 1.5 and 15 cm^{-1}, respectively (Fig. 10 *A*). These values are indicative of highly ordered chains for both CerIII and PA-d_{31}. They were indeed coherent with the overall behavior reported in Fig. 4. On heating at 45°C and above, the distribution of I_{2880}/I_{2850} ratios was progressively shifted toward lower values, and a relatively narrow distribution centered at ~0.95 was obtained at 75°C. This shift was associated with the disordering of the CerIII acyl chain during the transition. By contrast, the $\Delta\nu_{CD}$ spatial distribution remained fairly unchanged on heating up to 75°C, another indication of the high order experienced by the PA-d_{31} in the CerIII/PA-d_{31}/chol mixture

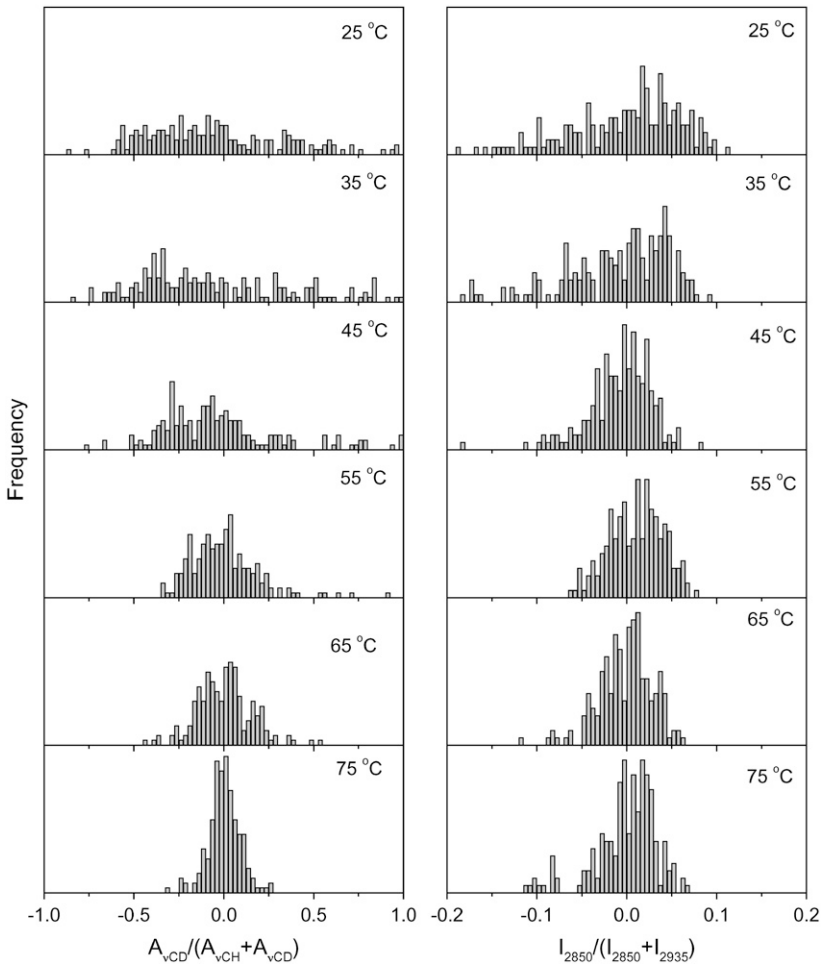

FIGURE 8 Normalized lipid spatial distributions in the CerIII/PA-d_{31}/CS (1:1:1) mixtures with 100 mM Ca^{2+}. (*Left*) $A_{\nu CD}/(A_{\nu CD} + A_{\nu CH})$ representing the distribution of PA-d_{31} relative to (CerIII/PA-d_{31}/CS). (*Right*) $I_{2850}/(I_{2850} + I_{2935})$ representing the distribution of CerIII relative to (CerIII/CS). The *y*-scale was kept the same for the parameter distributions at different temperatures.

in the presence of Ca^{2+}. It should be observed that the $\Delta\nu$CD distribution became slightly wider at high temperature with some values as high as 25 cm^{-1}. Fig. 10 *B* displays the distributions of the two parameters for the CerIII/PA-d_{31}/CS mixtures in the presence of 100 mM Ca^{2+}. At low temperature, these distributions were similar to those obtained with CerIII/PA-d_{31}/chol mixtures and were indicative of highly ordered acyl chains for both lipid species. Both parameter distributions shifted correspondingly when the samples were heated at 45°C and above, to reach values that were typical of disordered chains. This change reflected the disordering of both CerIII and PA-d_{31} associated with the transitions. A similar behavior was observed for both mixtures in the absence of Ca^{2+} (data not shown).

Chemical maps describing the chain order, derived from I_{2880}/I_{2850} and $\Delta\nu$CD, are presented in Fig. 11. The scale was selected to provide bright colors for values corresponding to disordered acyl chains. For the CerIII/PA-d_{31}/chol mixture in the presence of Ca^{2+} (Fig. 11 *A*), the values of the I_{2880}/I_{2850} ratios were fairly uniform over the map and representative of ordered CerIII acyl chains. On heating, a progressive decrease of these ratio values was experienced relatively uniformly over the map. At high temperatures, the majority of the pixels are green, indicative of disordered CerIII over the whole sample. The PA-d_{31} chain order was high at 25°C, as expressed by the low values of $\Delta\nu_{CD}$ (*dark pixels*). On heating, the chain order of the fatty acid became more heterogeneous, as inferred above from the histograms of Fig. 10 *A*. The maps at high temperatures showed that most of PA-d_{31} remained ordered, as illustrated by a dark background. However, in a few sampling elements, there was a considerable disordering of the PA-d_{31} acyl chains, represented by bright red pixels. These disordered PA-d_{31} molecules were found to be distributed mainly in regions depleted in PA-d_{31} or, in other words, enriched in CerIII and/or cholesterol. This colocalization was particularly obvious for the CerIII/chol-enriched domain (Fig. 9 *A*) and the disordered PA-d_{31} domain (Fig. 11 *A*) in the bottom left corner. Fig. 11 *B* illustrates, as a reference, the progressive and more uniform chain disordering of both PA and CerIII in the CerIII/PA-d_{31}/CS mixture in the presence of Ca^{2+}.

DISCUSSION

First, the work presented here reveals the thermal evolution of the microscopic domains that were previously observed in

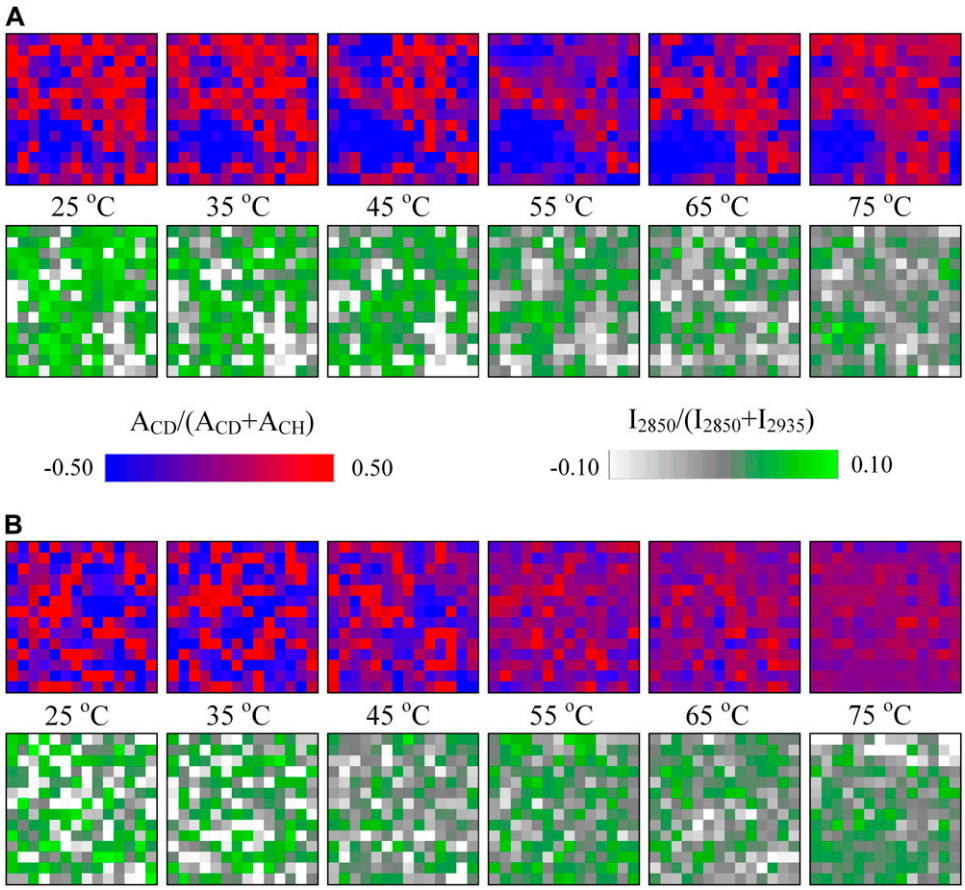

FIGURE 9 Chemical maps representing the normalized lipid spatial distribution in the CerIII/PA-d_{31}/sterol (1:1:1) mixtures with 100 mM Ca^{2+}. (*A*) Cholesterol-containing mixture. (*B*) CS-containing mixture. (*Top*) $A_{\nu CD}/(A_{\nu CD} + A_{\nu CH})$ representing the distribution of PA-d_{31} relative to (CerIII/PA-d_{31}/sterol). (*Bottom*) $I_{2850}/(I_{2850} + I_{2935})$ representing the distribution of CerIII relative to (CerIII/sterol).

CerIII/PA-d_{31}/chol mixtures at room temperature. It has been established that CerIII/PA-d_{31}/chol mixtures at low temperatures display crystalline domains with orthorhombic chain packing formed independently by CerIII and PA-d_{31} (27,28,41,48). On heating, there is a phase transition around 45–55°C, leading to the formation of a lamellar liquid ordered phase (27–29,49). This phase includes PA-d_{31}, cholesterol, and some CerIII. The involvement of CerIII in this phase is reported, for example, by the shift of the ν_{CH} position in the IR spectra ((27) and this work), and the decrease of the first moment of the ^{1}H-NMR spectra (55) of the CerIII/PA-d_{31}/chol mixtures. The overall behavior obtained by Raman spectroscopy confirms that both PA-d_{31} and CerIII are involved in this transition because the I_{2880}/I_{2850} intensity ratio, and the $\Delta\nu_{CD}$ both reported the concomitant disordering of the acyl chains of CerIII and PA-d_{31}. Further heating induces another transition, leading to a disordered phase, in which PA-d_{31} displays isotropic motions on the ^{2}H-NMR time scale (10^{-5} s) (29,49,55). The Raman chemical mapping presented here confirms the composition heterogeneity in the CerIII/PA-d_{31}/cholesterol mixture observed at low temperature (42,45) because the spatial distributions of PA-d_{31} and of CerIII, illustrated by the histograms in Fig. 5, are broad in these conditions. The present work confirms that, in addition to the chain disordering previously reported, the transition observed at 45–55°C involves a redistribution of PA-d_{31}, CerIII, and cholesterol in the SC lipid matrix and that the mixtures become more homogeneous on the microscopic scale. On heating above 45°C, homogenization of the spatial distribution of the lipids is observed for both PA-d_{31}, relative to the three lipid species, and CerIII, relative to (CerIII + chol), the composition distributions becoming considerably narrower. This homogenization happens at least at the microscopic scale, the size of a sampling element being estimated to $2 \times 2 \times 5\ \mu m^3$. The existence of smaller domains cannot, however, be excluded. Therefore, the results indicate that the SC model lipid mixture undergoes a phase transition where, at low temperatures, lipids form mainly a mosaic of microcrystalline phase-separated domains, and above 45°C, a more fluid and disordered phase where the three lipid species are more miscible is formed. Associated with these different structures, it is believed that the low- and the high-temperature organizations have different mechanical properties and cohesion. The modulation of this lipid phase transition provides a practical and efficient approach to change the functions of this material. Ca^{2+} and CS can play a role in such modulation.

The presence of Ca^{2+} modifies to a great extent the phase behavior of CerIII/PA-d_{31}/chol mixture. The major molecular feature of this effect is that, as clearly indicated by IR

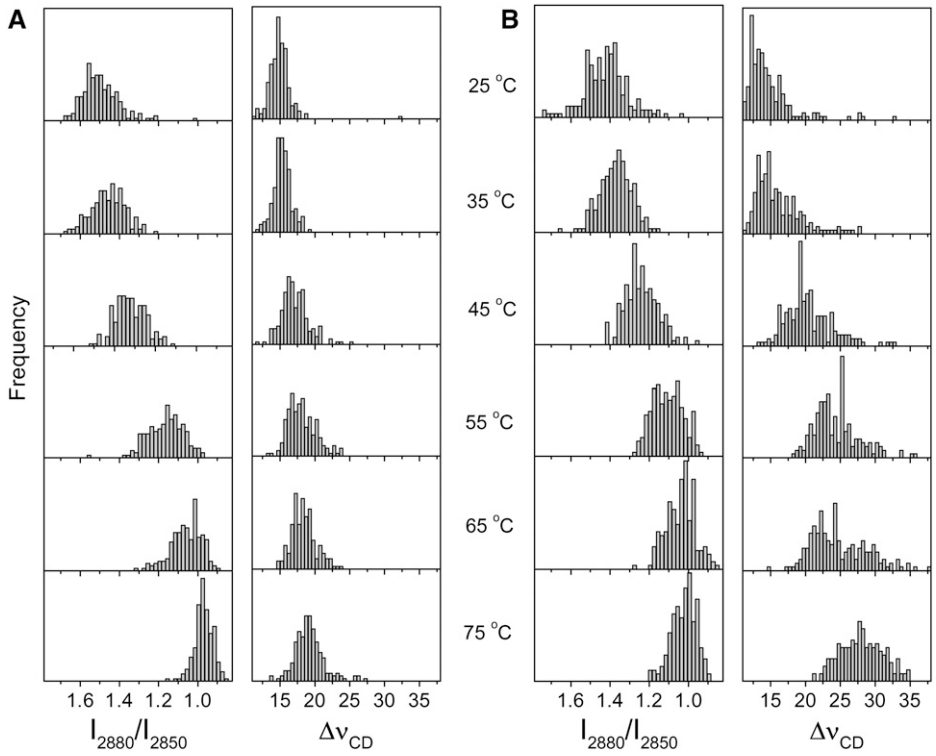

FIGURE 10 Spatial distributions of the acyl chain order in CerIII/PA-d_{31}/sterol (1:1:1) mixtures with 100 mM Ca^{2+}. The CerIII chain order is described using the I_{2880}/I_{2850} ratio, whereas that of PA-d_{31} is probed using $\Delta\nu_{CD}$. (*A*) Cholesterol-containing mixture. (*B*) CS-containing mixture. The *y*-scale was kept the same for the parameter distributions at different temperatures.

spectroscopy, Ca^{2+} displaces the proton of PA-d_{31} to form a complex with the carboxylate group. The fatty acid-Ca^{2+} association has never been demonstrated, to our knowledge, for SC lipid models, even though complexes with Ca^{2+} have been reported for simple systems formed of fatty acids (64,72,73) and for systems including negatively charged phospholipids (74–77). It has been shown that the apparent pK_a of PA-d_{31} inserted in CerIII/PA-d_{31}/chol mixture was ~7.0 (78), a value similar to those reported for analogous mixtures (57). This value is indeed much higher than that observed for monomeric fatty acid, for which an apparent pK_a of ~4.8 is reported (79,80). This difference was proposed to be associated with the pH gradient from the bulk to the membrane interface that led to a lower interfacial pH and putative interactions between the carboxylic group with other components of the bilayers, including cholesterol (81,82). From the apparent pK_a, it can be estimated that most of the PA-d_{31} molecules in CerIII/PA-d_{31}/chol mixtures were protonated at pH 5.2: this prediction is validated by the IR spectra. In the presence of Ca^{2+}, the IR results shown here indicate that the carboxylate groups act as complexation sites for the cations. Therefore, an interfacial equilibrium exists among R-COOH, R-COO^-, and R-COO-Ca^{2+}. The proportion of R-COO^- is likely negligible, assuming that the apparent pK_a of the fatty acid remains similar to that measured in the absence of Ca^{2+}. Moreover, the IR signal detected in the region between 1500, and 1600 cm^{-1} is indicative of the Ca^{2+}-PA complexation (62–65). This complexation leads to the formation of stable solid microscopic domains and prevents the thermal disordering of the PA-d_{31} acid chains. This is observed from both the absence of shift of the ν_{CD} band in the IR spectra (Fig. 1 *B*) and broadening of the ν_{CD} in the Raman spectra (Figs. 4 *B* and 10 *A*). As a consequence, the CerIII/PA-d_{31}/chol mixture remains phase-separated in the presence of Ca^{2+} even up to 75°C, as observed for example in Figs. 6 and 9. The association of Ca^{2+} to negatively charged lipids has been shown to lead to structures that are stable over a wide temperature interval (65,83,84). Our results show that an analogous phenomenon takes place in SC model lipid matrices.

The complexation of PA with Ca^{2+} modifies the thermotropism of the CerIII/PA-d_{31}/chol mixtures. Because most of the PA molecules are no longer available to participate in the order-disorder transitions, the CerIII acyl chain disordering is shifted toward high temperatures. In these conditions, the more fluid and disordered phase resulting from the transition between 40 and 50°C must be predominantly composed of CerIII and cholesterol. It was previously reported that binary CerIII/chol mixtures (without Ca^{+2}) undergo a transition, at ~55°C, from a crystalline phase with orthorhombic chain packing to a more disordered phase (41), which is likely a liquid ordered phase. A similar behavior was also observed for the mixtures of cholesterol with CerIV, an α-hydroxy ceramide (85). In these binary systems, a cholesterol mole fraction of 0.6–0.75 was required for the involvement of all the ceramide molecules in the transition. In our model mixtures, this fraction was 0.5 if one considers strictly CerIII and cholesterol, leading probably to solid

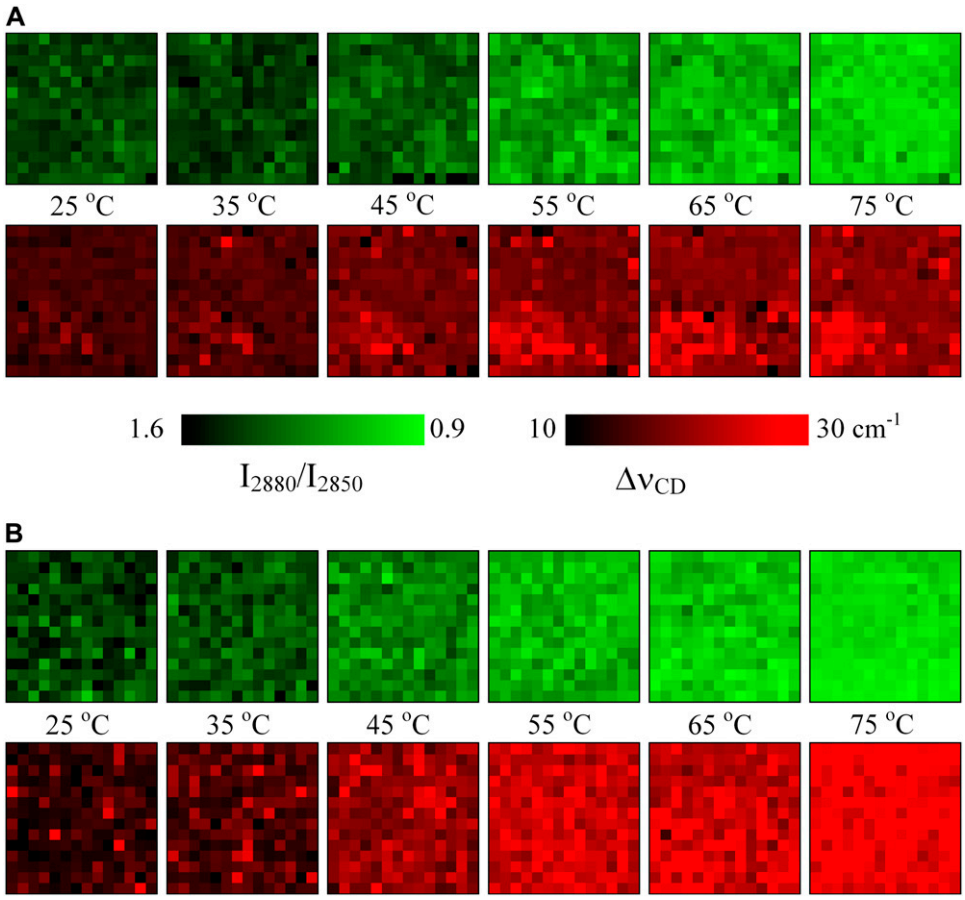

FIGURE 11 Chemical maps representing the spatial distribution of the acyl chain order in CerIII/PA-d_{31}/sterol (1:1:1) mixtures with 100 mM Ca^{2+}. (*A*) Cholesterol-containing mixture. (*B*) CS-containing mixture. The CerIII chain order is described using the I_{2880}/I_{2850} ratio (*top*), whereas that of PA-d_{31} is probed using $\Delta\nu_{CD}$ (*bottom*).

ceramide, corresponding to the fraction in excess. It is therefore proposed that the disordering of the ceramide acyl chains observed at ~45°C, from the vibrational spectroscopic probes presented here, corresponds to the formation of a liquid ordered phase by a fraction of the CerIII and cholesterol. This fluid phase should also include some PA molecules because, even with the present Ca^{2+} concentration, some acid remains uncomplexed. This would be at the origin of the shift of the order-disorder transition observed at ~45°C for the CerIII/PA-d_{31}/chol mixtures in the presence of Ca^{2+}, compared to ~55°C for binary mixtures made of ceramide and cholesterol. The disordering of some PA acyl chain is actually confirmed by the histograms (Fig. 10 *A*) and the maps (Fig. 11 *A*). In fact, it is found that the location of the small fraction of more disordered PA corresponds to regions depleted in PA or, in other words, enriched in CerIII and cholesterol. As an illustration, this colocalization is evident when one observes the PA-depleted domain in the left bottom corner of the high-temperature maps (Fig. 10) and the domain at the same position where PA acyl chains are more disordered in Fig. 11. When these samples are heated to a higher temperature, the CerIII chains experience, on average, an increased disordering. In agreement with previous observations on binary systems (41,85), this phenomenon is likely related to the excess CerIII, which remained solid because of the limited cholesterol proportion, that becomes progressively incorporated into the fluid phase. The present work reveals that the concentration of Ca^{2+} is a simple way to modulate the phase-mixing properties as well as the chain order of SC lipids, by controlling the proportion of PA available to participate in the temperature-induced disordering.

In the absence of Ca^{2+}, the spectroscopic results presented here suggest that CerIII/PA-d_{31}/CS mixture displays an analogous similar behavior to that of CerIII/PA-d_{31}/chol mixture. At low temperatures, both CerIII and PA-d_{31} display high acyl chain order, and they appear to be distributed inhomogeneously (Fig. 9). On heating, similar spectral changes could be observed, and it is likely that the systems undergo a transition from a highly ordered (solid) phase to a liquid ordered phase and then to a disordered phase. It has been shown that CS would influence phospholipid bilayers in a similar manner as cholesterol does, the main common feature being the ability of these sterols to abolish the gel-to-fluid phase transition (86,87). CS was found, however, to induce a less pronounced ordering of the fluid phospholipid acyl chains than cholesterol for a given sterol content. Despite several similarities reported here, it should be pointed out that CerIII/PA-d_{31}/CS and CerIII/PA-d_{31}/chol mixtures were macroscopically different at room temperature. The physical aspect of the samples of the CerIII/PA-d_{31}/CS mixtures,

which were opalescent white homogeneous suspensions, contrasted with the waxy particles obtained with CerIII/PA-d_{31}/chol mixtures. In addition, despite the highly ordered acyl chains inferred from the ν_{CH}, and ν_{CD} positions and the profiles of the ν_{COOH} and ν_{AmideI} regions typical of high order, the δ_{CH2} and δ_{CD2} bands did not show crystalline splittings as extensive as those observed in the case of CerIII/PA-d_{31}/chol mixture (data not shown). These splittings are indicative of crystalline structures with orthorhombic chain packing (48,88,89). It appears that the presence of CS would hinder the formation of such crystalline domains. This phenomenon is consistent with a previous study indicating that the presence of CS reduces the formation of cholesterol crystalline domains in SC model mixtures, as inferred from small-angle x-ray diffraction (34). Despite the limited presence of crystalline domains with orthorhombic chain packing, the CerIII/PA-d_{31}/CS mixtures investigated here appeared to maintain, at low temperatures, a very high acyl chain order and a heterogeneous spatial distribution.

The replacement of cholesterol by CS has a major impact when the SC model mixtures are in the presence of Ca^{2+}. A striking feature is that most PA-d_{31} does not complex with Ca^{2+}. It is possible that, in these mixtures, the sulfate groups become the new binding sites for the cations. This could be associated with the readily available negative charge on the sterol molecule. A significant consequence of this change is the involvement of the PA-d_{31} molecules in the phase transitions induced by heating. In fact, the behavior of CerIII/PA-d_{31}/CS mixture in the presence of Ca^{2+} is analogous to that observed for CerIII/PA-d_{31}/CS mixture and CerIII/PA-d_{31}/chol mixture in the absence of Ca^{2+}. This suggests that the three lipid species are involved in the phase transitions observed on heating. It also indicates that CS preserves its ability to induce the formation of fluid phases despite its putative interactions with Ca^{2+}.

In the work presented here, the modifications were induced by somewhat drastic changes: the complete replacement of cholesterol by CS and the presence of 100 mM Ca^{2+}. These are indeed severe conditions that were used to unmistakably highlight the changes induced by these species. The complexation of Ca^{2+} with the carboxylate group of fatty acids and the modulation of this complexation by CS were manifest in the spectra. At 100 mM, Ca^{2+} complexed the majority of the fatty acid molecules, which remained solid and phase-separated over the whole investigated temperature range. These equilibria are defined by the local concentrations of these chemical species. Even though their shifts are likely to be not as pronounced in real SC, the equilibria presented here must exist and provide an efficient and relatively simple way to modulate the properties of SC that could be used in vivo. The Ca^{2+} ion concentration is proposed to peak at the level of the stratum granulosum (39). In parallel, the epidermis begins to produce free fatty acids and CS at this level (3). Actually, the Ca^{2+} gradient across the epidermis is reminiscent of that of CS (33). These coinciding gradients suggest that their combined effects modulate the lipid matrix properties across the epidermis, having in mind the impacts presented here. Now that the nature of the interactions has been identified, the next step is to assess how these impacts are extrapolated to more physiologically relevant concentrations, using the probes discussed here. In addition, the reported phenomena must be examined on more complex systems because one should keep in mind that the SC model mixtures used here are simplified systems that imperfectly reproduce the behavior of real SC. For example, it will be interesting to infer the influence of the different types of ceramides and the presence of the long-periodicity phase on the present findings.

The work presented here reveals that CS and Ca^{2+} modulate the lipid mixing properties and the lipid order in SC lipid models. As a consequence, several properties of the SC that are believed to be associated with the lipid phase behavior, including permeability and desquamation, could be efficiently modulated by the concentration of these species. For example, Ca^{2+} displayed fusogenic power on large unilamellar vesicles formed with ceramides, fatty acids, and sterols (90,91). The intervesicle lipid mixing observed in the presence of Ca^{2+} was associated with the formation of the lamellar sheets at the stratum granulosum level. This activity of Ca^{2+} was inhibited by the presence of CS in the vesicles. On the basis of the results presented here, it is possible that a shift of the equilibria involving Ca^{2+} and the fatty acids is at the origin of this control of the bilayer fusion. Such modulation of the Ca^{2+} equilibria involving CS and fatty acids would suggest a potential role in inter–lipid bilayer interactions in the epidermis. Along the same line, the excessive cohesion of SC in the case of the X-linked recessive ichthyosis has been associated with the accumulation of CS (5,7,33). The bridging of CS by Ca^{2+} ions (92) and the different mixing properties of cholesterol and CS (40,93) have been proposed as possible molecular mechanisms involved in the excessive cohesion of the SC. As a complementary or alternative mechanism, one could consider that the higher CS content limits the complexation of Ca^{2+} with the fatty acids in the deep layers of SC and prevents the formation of very stable and ordered phase-separated domains. This could lead to more homogeneous and likely more cohesive lipid matrices. Such a hypothesis is somehow supported by the increased cholesterol solubility in the presence of CS in SC model mixtures containing 2 mM Ca^{2+} (34), considering that ''free'' palmitic acid favors the solubilization of cholesterol in fluid ceramide bilayers (41). On the basis of the findings reported here, the fine balance of the equilibria among Ca^{2+}, fatty acid, and CS should be further investigated to examine its impact on the organization and the function of the epidermis.

The authors thank the Natural Sciences and Engineering Research Council (Canada) for the Collaborative Health Research Project funding. M.A. is grateful to Fonds Québécois de la Recherche sur la Nature et les

Technologies (FQRNT) (Quebec) for her scholarship. This work was also funded by FQRNT through its financial support to the Center for Self-Assembled Chemical Systems.

REFERENCES

1. Elias, P. M., G. K. Menon, S. Grayson, and B. E. Brown. 1988. Membrane structural alterations in murine stratum corneum: relationship to the localization of polar lipids and phospholipases. *J. Invest. Dermatol.* 91:3–10.
2. Yardley, H. J., and R. Summerly. 1981. Lipid composition and metabolism in normal and diseased epidermis. *Pharmacol. Ther.* 13: 357–383.
3. Elias, P. M. 1983. Epidermal lipids, barrier function, and desquamation. *J. Invest. Dermatol.* 80:44s–49s.
4. Milstone, L. M. 2004. Epidermal desquamation. *J. Dermatol. Sci.* 36: 131–140.
5. Williams, M. L. 1991. Lipids in normal and pathological desquamation. *Adv. Lipid Res.* 24:211–262.
6. Elias, P. M., and G. K. Menon. 1991. Structural and lipid biochemical correlates of the epidermal permeability barrier. *Adv. Lipid Res.* 24: 1–26.
7. Williams, M. L., S. Grayson, J. M. Bonifas, E. H. Epstein Jr., and P. M. Elias. 1983. Epidermal cholesterol sulfate and steroid sulfatase activity and recessive X-linked ichthyosis. *In* The Stratum Corneum. R. Marks and O. Plewid, editors. Springer-Verlag, Heidelberg. 79–85.
8. Vičanová, J., E. Boelsma, M. A. Mommaas, J. A. Kempenaar, B. Forslind, J. Pallon, T. Elgerud, H. K. Koerten, and M. Ponec. 1998. Normalization of epidermal calcium distribution profile in reconstructed human epidermis is related to improvement of terminal differentiation and stratum corneum barrier formation. *J. Invest. Dermatol.* 111:97–106.
9. Tanojo, H., and H. I. Maibach. 1999. Role of calcium ions in relation to skin barrier function. *Drugs Pharm. Sci.* 97:939–950.
10. Barbotteau, Y., E. Gontier, P. Barberet, M. Cappadoro, B. De Wever, C. Habchi, S. Incerti, A. Mavon, P. Moretto, T. Pouthier, R. W. Smith, and M. D. Ynsa. 2005. Reconstructed human epidermis: a model to study the barrier function. *Nucl. Instrum. Methods Phys. Res. B.* 231: 286–291.
11. Mauro, T., G. Bench, E. Sidderas-Haddad, K. Feingold, P. Elias, and C. Cullander. 1998. Acute barrier perturbation abolishes the Ca^{2+} and K^{+} gradients in murine epidermis: quantitative measurement using PIXE. *J. Invest. Dermatol.* 111:1198–1201.
12. Elias, P. M., S. K. Ahn, B. E. Brown, D. Crumrine, and K. R. Feingold. 2002. Origin of the epidermal calcium gradient: regulation by barrier status and role of active vs. passive mechanisms. *J. Invest. Dermatol.* 119:1269–1274.
13. Schurer, N. Y., and P. M. Elias. 1991. The biochemistry and function of stratum corneum lipids. *Adv. Lipid Res.* 24:27–56.
14. Wertz, P. W., and D. T. Downing. 1989. Stratum corneum: biological and biochemical considerations. *Transderm. Drug Deliv.* 35:1–22.
15. Wertz, P. W., M. C. Miethke, S. A. Long, J. S. Strauss, and D. T. Downing. 1985. The composition of the ceramides from human stratum corneum and from comedones. *J. Invest. Dermatol.* 84:410–412.
16. Wertz, P. W., D. C. Swartzendruber, K. C. Madison, and D. T. Downing. 1987. Composition and morphology of epidermal cyst lipids. *J. Invest. Dermatol.* 89:419–425.
17. Nicollier, M., T. Massengo, J.-P. Rémy-Martin, R. Laurent, and G.-L. Adessi. 1986. Free fatty acids and fatty acids of triacylglycerols in normal and hyperkeratotic human stratum corneum. *J. Invest. Dermatol.* 87:68–71.
18. Lampe, M. A., A. L. Burlingame, J. Whitney, M. L. Williams, B. E. Brown, E. Roitman, and P. M. Elias. 1983. Human stratum corneum lipids: characterization and regional variation. *J. Lipid Res.* 24: 120–130.
19. Bouwstra, J. A., J. Thewalt, G. S. Gooris, and N. Kitson. 1997. A model membrane approach to the epidermal permeability barrier: an x-ray diffraction study. *Biochemistry.* 36:7717–7725.
20. Bouwstra, J. A., G. S. Gooris, J. A. van der Spek, and W. Bras. 1991. Structural investigations of human stratum corneum by small-angle x-ray scattering. *J. Invest. Dermatol.* 97:1005–1012.
21. Bouwstra, J. A., G. S. Gooris, M. A. Salomons-de Vries, J. A. van der Spek, and W. Bras. 1992. Structure of human stratum corneum as a function of temperature and hydratation: a wide-angle x-ray diffraction study. *Int. J. Pharm.* 84:205–216.
22. Bouwstra, J. A., G. S. Gooris, J. van der Spek, S. Lavvrijsen, and W. Bras. 1994. The lipid and protein structure of mouse stratum corneum: a wide and small angle diffraction study. *Biochim. Biophys. Acta.* 1212:183–192.
23. de Jager, M. W., G. S. Gooris, I. P. Dolbnya, W. Bras, M. Ponec, and J. A. Bouwstra. 2004. Novel lipid mixtures based on synthetic ceramides reproduce the unique stratum corneum lipid organization. *J. Lipid Res.* 45:923–932.
24. de Jager, M. W., G. S. Gooris, I. P. Dolbnya, M. Ponec, and J. A. Bouwstra. 2004. Modelling the stratum corneum lipid organisation with synthetic lipid mixtures: the importance of synthetic ceramide composition. *Biochim. Biophys. Acta.* 1684:132–140.
25. de Jager, M., G. S. Gooris, M. Ponec, and J. A. Bouwstra. 2005. Lipid mixtures prepared with well-defined synthetic ceramides closely mimic the unique stratum corneum lipid phase behavior. *J. Lipid Res.* 46: 2649–2656.
26. Parrott, D. T., and J. E. Turner. 1993. Mesophase formation by ceramides and cholesterol: a model for stratum corneum lipid packing? *Biochim. Biophys. Acta.* 1147:273–276.
27. Lafleur, M. 1998. Phase behaviour of model stratum corneum lipid mixtures: an infrared spectroscopy investigation. *Can. J. Chem.* 76: 1501–1511.
28. Moore, D. J., M. E. Rerek, and R. Mendelsohn. 1997. Lipid domains and orthorhombic phases in model stratum corneum: evidence from Fourier transform infrared spectroscopy studies. *Biochem. Biophys. Res. Commun.* 231:797–801.
29. Kitson, N., J. Thewalt, M. Lafleur, and M. Bloom. 1994. A model approach to the epidermal permeability barrier. *Biochemistry.* 33: 6707–6715.
30. Potts, R. O., and M. L. Francoeur. 1993. Infrared spectroscopy of stratum corneum lipids. *Drugs Pharm. Sc.* 59:269–291.
31. Ongpipattanakul, B., M. L. Francoeur, and R. O. Potts. 1994. Polymorphism in stratum corneum lipids. *Biochim. Biophys. Acta.* 1190:115–122.
32. Bouwstra, J. A., G. S. Gooris, K. Cheng, A. M. Weerheim, W. Bras, and M. Ponec. 1996. Phase behavior of isolated skin lipids. *J. Lipid Res.* 37:999–1011.
33. Zettersten, E., M.-Q. Man, J. Sato, M. Denda, A. Farrell, R. Ghadially, M. L. Williams, K. R. Feingold, and P. M. Elias. 1998. Recessive X-linked ichthyosis: role of cholesterol-sulfate accumulation in the barrier abnormality. *J. Invest. Dermatol.* 111:784–790.
34. Bouwstra, J. A., G. S. Gooris, F. E. R. Dubbelaar, and M. Ponec. 1999. Cholesterol sulfate and calcium affect stratum corneum lipid organization over a wide temperature range. *J. Lipid Res.* 40:2303–2312.
35. Elias, P. M., D. Crumrine, U. Rassner, J.-P. Hachem, G. K. Menon, W. Man, M. H. W. Choy, L. Leypoldt, K. R. Feingold, and M. L. Williams. 2004. Basis for abnormal desquamation and permeability barrier dysfunction in RXLI. *J. Invest. Dermatol.* 122:314–319.
36. Weerheim, A., and M. Ponec. 2001. Determination of stratum corneum lipid profile by tape stripping in combination with high-performance thin-layer chromatography. *Arch. Dermatol. Res.* 293:191–199.
37. Lee, S. H., E. H. Choi, K. R. Feingold, S. Jiang, and S. K. Ahn. 1998. Iontophoresis itself on hairless mouse skin induces the loss of the epidermal calcium gradient without skin barrier impairment. *J. Invest. Dermatol.* 111:39–43.
38. Elias, P. M., P. Nau, K. Hanley, C. Cullander, D. Crumrine, G. Bench, E. Sideras-Haddad, T. Mauro, M. L. Williams, and K. R. Feingold.

1998. Formation of the epidermal calcium gradient coincides with key milestones of barrier ontogenesis in the rodent. *J. Invest. Dermatol.* 110:399–404.

39. Menon, G. K., S. Grayson, and P. M. Elias. 1985. Ionic calcium reservoirs in mammalian epidermis: ultrastructural localization by ion-capture cytochemistry. *J. Invest. Dermatol.* 84:508–512.
40. Rehfeld, S. J., W. Z. Plachy, M. L. Williams, and P. M. Elias. 1988. Calorimetric and electron spin resonance examination of lipid phase transitions in human stratum corneum: molecular basis for normal cohesion and abnormal desquamation in recessive X-linked ichthyosis. *J. Invest. Dermatol.* 91:499–505.
41. Velkova, V., and M. Lafleur. 2002. Influence of the lipid composition on the organization of skin lipid model mixtures: an infrared spectroscopy investigation. *Chem. Phys. Lipids.* 117:63–74.
42. Mendelsohn, R., and D. J. Moore. 2000. Infrared determination of conformational order and phase behavior in ceramides and stratum corneum models. *Methods Enzymol.* 312:228–247.
43. Moore, D. J., and M. E. Rerek. 2000. Insights into the molecular organization of lipids in the skin barrier from infrared spectroscopy studies of stratum corneum lipid models. *Acta Derm. Venereol. Suppl. (Stockh.).* 208:16–22.
44. Moore, D. J., M. E. Rerek, and R. Mendelsohn. 1997. FTIR spectroscopy studies of the conformational order and phase behavior of ceramides. *J. Phys. Chem. B.* 101:8933–8940.
45. Percot, A., and M. Lafleur. 2001. Direct observation of domains in model stratum corneum lipid mixtures by Raman microspectroscopy. *Biophys. J.* 81:2144–2153.
46. Wilhelm, D., P. Elsner, and H. I. Maibach. 1991. Standardized trauma (tape stripping) in human vulvar and forearm skin, effects on transepidermal water loss, capacitance and pH. *Acta Derm. Venereol.* 71:123–126.
47. Ohman, H., and A. Vahlquist. 1994. In vivo studies concerning a pH gradient in human stratum corneum and upper epidermis. *Acta Derm. Venereol.* 74:375–379.
48. Moore, D. J., R. G. Snyder, M. E. Rerek, and R. Mendelsohn. 2006. Kinetics of membrane raft formation: fatty acid domains in stratum corneum lipid models. *J. Phys. Chem. B.* 110:2378–2386.
49. Fenske, D. B., J. L. Thewalt, M. Bloom, and N. Kitson. 1994. Model of stratum corneum intercellular membranes: ^{2}H NMR of macroscopically oriented multilayers. *Biophys. J.* 67:1562–1573.
50. Mantsch, H. H., and R. N. McElhaney. 1991. Phospholipid phase transitions in model and biological membranes as studied by infrared spectroscopy. *Chem. Phys. Lipids.* 57:213–226.
51. Kodati, V. R., R. El-Jastimi, and M. Lafleur. 1994. Contribution of the intermolecular coupling and librotorsional mobility in the methylene stretching modes in the infrared spectra of acyl chains. *J. Phys. Chem.* 98:12191–12197.
52. Kodati, R. V., and M. Lafleur. 1993. Comparison between orientational and conformational orders in fluid lipid bilayers. *Biophys. J.* 64:163–170.
53. Paré, C., and M. Lafleur. 2001. Formation of liquid ordered lamellar phases in the palmitic acid/cholesterol system. *Langmuir.* 17:5587–5594.
54. Silvius, J. R., D. del Giudice, and M. Lafleur. 1996. Cholesterol at different bilayer concentrations can promote or antagonize lateral segregation of phospholipids of differing acyl chain length. *Biochemistry.* 35:15198–15208.
55. Thewalt, J., N. Kitson, C. Araujo, A. MacKay, and M. Bloom. 1992. Models of stratum corneum intercellular membranes: the sphingolipid headgroup is a determinant of phase behavior in mixed lipid dispersions. *Biochem. Biophys. Res. Commun.* 188:1247–1252.
56. Lieckfeldt, R., J. Villalaín, J.-C. Gómez-Fernández, and G. Lee. 1994. Influence of oleic acid on the structure of a mixture of hydrated model stratum corneum fatty acids and their soaps. *Colloids Surf. A.* 90:225–234.
57. Lieckfeldt, R., J. Villalaín, J.-C. Gómez-Fernández, and G. Lee. 1995. Apparent pK_a of the fatty acids within ordered mixtures of model human stratum corneum lipids. *Pharm. Res.* 12:1614–1617.
58. Cevc, G., J. M. Seddon, R. Hartung, and W. Eggert. 1988. Phosphatidylcholine-fatty acid membranes. I. Effects of protonation, salt concentration, temperature and chain-length on the colloidal and phase properties of mixed vesicles, bilayers and nonlamellar structures. *Biochim. Biophys. Acta.* 940:219–240.
59. Ouimet, J., and M. Lafleur. 2004. Hydrophobic match between cholesterol and saturated fatty acid is required for the formation of lamellar liquid ordered phases. *Langmuir.* 20:7474–7481.
60. Gómez-Fernández, J. C., and J. Villalaín. 1998. The use of FT-IR for quantitative studies of the apparent pKa of lipid carboxyl groups and the dehydration degree of the phosphate group of phospholipids. *Chem. Phys. Lipids.* 96:41–52.
61. Ouimet, J., S. Croft, C. Paré, J. Katsaras, and M. Lafleur. 2003. Modulation of the polymorphism of the palmitic acid/cholesterol system by the pH. *Langmuir.* 19:1089–1097.
62. Lu, Y., and J. D. Miller. 2002. Carboxyl stretching vibrations of spontaneously adsorbed and LB-transferred calcium carboxylates as determined by FTIR internal reflection spectroscopy. *J. Colloid Interface Sci.* 256:41–52.
63. Marshbanks, T. L., and E. I. Franses. 1994. Transport and ion-exchange dynamics in Langmuir-Blodgett films of fatty acids. *J. Phys. Chem.* 98:2166–2173.
64. Bagg, J., M. B. Abramson, M. Fichman, M. D. Haber, and H. P. Gregor. 1964. Composition of stearic acid monolayers from calcium-containing substrates. *J. Am. Chem. Soc.* 86:2759–2763.
65. MacDonald, R. C., S. A. Simon, and E. Baer. 1976. Ionic influences on the phase transition of dipalmitoylphosphatidylserine. *Biochemistry.* 15:885–891.
66. Bunow, M. R., and I. W. Levin. 1977. Comment on the carbon-hydrogen stretching region of vibrational Raman spectra of phospholipids. *Biochim. Biophys. Acta.* 487:388–394.
67. Huang, C., J. T. Mason, and I. W. Levin. 1983. Raman spectroscopic study of saturated mixed-chain phosphatidylcholine multilamellar dispersions. *Biochemistry.* 22:2775–2780.
68. Mendelsohn, R., and C. C. Koch. 1980. Deuterated phospholipids as Raman spectroscopic probes of membrane structure. *Biochim. Biophys. Acta.* 598:260–271.
69. Gaber, B. P., and W. L. Peticolas. 1977. On the quantitative interpretation of biomembrane structure by Raman spectroscopy. *Biochim. Biophys. Acta.* 465:260–274.
70. Levin, I. W. 1984. Vibrational spectroscopy of membrane assemblies. *Adv. Infrared Raman Spectrosc.* 11:1–48.
71. Kouaouci, R., J. R. Silvius, I. Graham, and M. Pézolet. 1985. Calcium-induced lateral phase separation in phosphatidylcholine-phosphatidic acid mixtures. A Raman spectroscopic study. *Biochemistry.* 24:7132–7140.
72. Hauser, H., W. Guyer, and K. Howell. 1979. Lateral distribution of negatively charged lipids in lecithin membranes. Clustering of fatty acids. *Biochemistry.* 18:3285–3291.
73. Deamer, D. W., D. W. Meek, and D. G. Cornwell. 1967. Properties, composition, and structure of stearic acid-stearate monolayers on alkaline earth solutions. *J. Lipid Res.* 8:255–263.
74. Van Dijck, P. W. M., B. De Kruijff, A. J. Verkleij, L. L. M. Van Deenen, and J. De Gier. 1978. Comparative studies on the effects of pH and Ca^{2+} on bilayers of various negatively charged phospholipids and their mixtures with phosphatidylcholine. *Biochim. Biophys. Acta.* 512:84–96.
75. Laroche, G., E. J. Dufourc, J. Dufourcq, and M. Pézolet. 1991. Structure and dynamics of dimyristoylphosphatidic acid/calcium complexes by ^{2}H NMR, infrared, and Raman spectroscopies and small-angle x-ray diffraction. *Biochemistry.* 30:3105–3113.
76. Tilcock, C. P. S., M. B. Bally, S. B. Farren, P. R. Cullis, and S. M. Gruner. 1984. Cation-dependent segregation phenomena and phase behavior in model membrane systems containing phosphatidylserine: influence of cholesterol and acyl chain composition. *Biochemistry.* 23:2696–2703.
77. Papahadjopoulos, D., W. J. Vail, K. Jacobson, and G. Poste. 1975. Cochleate lipid cylinders: formation by fusion of unilamellar lipid vesicles. *Biochim. Biophys. Acta.* 394:483–491.

78. Velkova, V. 2000. Étude de l'effet de la composition et du pH sur le thermotropisme de mélanges lipidiques modèles du stratum corneum par spectroscopie infrarouge. Université de Montréal, Montréal.

79. Cistola, D. P., J. A. Hamilton, D. Jackson, and D. M. Small. 1988. Ionization and phase behaviour of fatty acid in water: application of the Gibbs phase rule. *Biochemistry.* 27:1881–1888.

80. Cistola, D. P., D. M. Small, and J. A. Hamilton. 1982. Ionization behavior of aqueous short-chain carboxylic acids: a carbon-13 NMR study. *J. Lipid Res.* 23:795–799.

81. Cistola, D. P., D. Atkinson, J. A. Hamilton, and D. M. Small. 1986. Phase behavior and bilayer properties of fatty acids: hydrated 1:1 acid-soaps. *Biochemistry.* 25:2804–2812.

82. McLaughlin, S. 1977. Electrostatic potentials at membrane-solution interfaces. *Curr. Top. Membr Transp.* 9:71–144.

83. Van Dijck, P. W. M., P. H. J. T. Ververgaert, A. J. Verkleij, L. L. M. Van Deenen, and J. De Gier. 1975. Influence of Ca^{2+} and Mg^{2+} on the thermotropic behaviour and permeability properties of liposomes prepared from dimyristoyl phosphatidylglycerol and mixtures of dimyristoyl phosphatidylglycerol and dimyristoyl phosphatidylcholine. *Biochim. Biophys. Acta.* 406:465–478.

84. Verkleij, A. J., B. De Kruyff, P. H. J. T. Ververgaert, J. F. Tocanne, and L. L. M. Van Deenen. 1974. The influence of pH, Ca^{2+} and protein on the thermotropic behaviour of the negatively charged phospholipid, phosphatidylglycerol. *Biochim. Biophys. Acta.* 339:432–437.

85. Wegener, M., R. Neubert, W. Rettig, and S. Wartewig. 1997. Structure of stratum corneum lipids characterized by FT-Raman spectroscopy and DSC. III. Mixtures of ceramides and cholesterol. *Chem. Phys. Lipids.* 88:73–82.

86. Le Grimellec, C., A. Daigneault, G. Bleau, and K. D. Roberts. 1984. Cholesteryl sulfate- phosphatidylcholine interactions. *Lipids.* 19: 474–477.

87. Kitson, N., M. Monck, K. Wong, J. Thewalt, and P. R. Cullis. 1992. The influence of cholesterol 3-sulphate on phase behaviour and hydrocarbon order in model membrane systems. *Biochim. Biophys. Acta.* 1111:127–133.

88. Mendelsohn, R., G. L. Liang, H. L. Strauss, and R. G. Snyder. 1995. IR spectroscopic determination of gel state miscibility in long-chain phosphatidylcholine mixtures. *Biophys. J.* 69:1987–1998.

89. Snyder, R. G., H. L. Strauss, and D. A. Cates. 1995. Detection and measurement of microaggregation in binary mixtures of esters and of phospholipid dispersions. *J. Phys. Chem.* 99:8432–8439.

90. Hatfield, R. M., and L. W.-M. Fung. 1999. A new model system for lipid interactions in stratum corneum vesicles: effects of lipid composition, calcium, and pH. *Biochemistry.* 38:784–791.

91. Abraham, W., P. W. Wertz, L. Landmann, and D. T. Downing. 1987. Stratum corneum lipid liposomes: calcium-induced transformation into lamellar sheets. *J. Invest. Dermatol.* 88:212–214.

92. Epstein, E. H., Jr., M. L. Williams, and P. M. Elias. 1981. Steroid sulfatase, X-linked ichthyosis, and stratum corneum cell cohesion. *Arch. Dermatol.* 117:761–763.

93. Rehfeld, S. J., M. L. Williams, and P. M. Elias. 1986. Interactions of cholesterol and cholesterol sulfate with free fatty acids: possible relevance for the pathogenesis of recessive X-linked ichthyosis. *Arch. Dermatol. Res.* 278:259–263.